J. Phys.: Condens. Matter **11** (1999) 4469–4481. Printed in the UK PII: S0953-8984(99)00379-3

Magnetic ordering of $Pr_6Fe_{13}Si$ and $Nd_6Fe_{13}Au$ studied by neutron diffraction

P Schobinger-Papamantellos†, K H J Buschow‡, C H de Groot‡, F R de Boer‡, Grit Böttger§ and C Ritter§

† Laboratorium für Kristallographie, ETHZ CH-8092 Zürich, Switzerland
‡ Van der Waals-Zeeman Institute, University of Amsterdam Valckenierstr. 65, 1018 XE Amsterdam, The Netherlands
§ Institut Laue–Langevin, 156X, 38042 Grenoble Cédex, France

Received 23 December 1998, in final form 29 March 1999

Abstract. The magnetic structure of the compounds $Pr_6Fe_{13}Si$ and $Nd_6Fe_{13}Au$ has been studied by powder neutron diffraction. The magnetic structures are very similar, revealing the same collinear antiferromagnetic ordering of the Fe (four) and the R (two) sublattices associated with the wavevector $\boldsymbol{q} = (001)$ and an I_P type magnetic lattice with anticentring translation. The moments of all sublattices located in $(xy0)$ layers and sandwiched between successive Si (Au) layers perpendicular to z at $z = -0.25$, 0.25, are confined to the same direction within the $(xy0)$ plane. They change their direction collectively when going to the next Au (Si) layers at $z = 0.25$, 0.75, thus producing antiferromagnetic ordering within all eight sublattices. At 1.5 K, the rare earth moments in $Nd_6Fe_{13}Au$ are equal to 3.4(2) μ_B for Nd1 and 2.5(1) μ_B for Nd2. In $Pr_6Fe_{13}Si$ the two Pr sites have almost the same moment of 2.8(1) μ_B at 1.5 K. The average ordered Fe moment value is lower in $Pr_6Fe_{13}Si$ (1.57 μ_B/Fe atom) than in $Nd_6Fe_{13}Au$ (2.3 μ_B/Fe atom).

1. Introduction

Rare earth compounds of the type $R_6Fe_{13}X$ are formed by combining light rare earths with X≡Cu, Ag, Au, Si or Sn. These compounds crystallize in the tetragonal $Nd_6Fe_{13}Si$ structure [1, 2] of space group $I4/mcm$ as an ordered variant of the $La_6Co_{11}Ga_3$ structure [3]. There are two rare earth sites, R_1 (8f) and R_2 (16l) and four Fe sites, Fe_1 (4d), Fe_2 (16k), Fe_3 ($16l_1$) and Fe_4 ($16l_2$). The magnetic properties of the $R_6Fe_{13}X$ compounds were studied by numerous authors [2, 4–12].

In several investigations it was found that magnetic ordering is characterized by a Néel-type transition at temperatures around 400 K [9–12] which was also confirmed by Mössbauer spectroscopy [7, 10]. The absence of a spontaneous magnetization of any significance at 4.2 K suggests that the magnetic structure consists of an antiferromagnetically ordered rare earth sublattice and an antiferromagnetically ordered Fe sublattice [9, 11]. For the compounds $Pr_6Fe_{13}Ag$ and $Pr_6Fe_{13}Au$ this was recently confirmed by neutron diffraction [8]. In fact, we found that the magnetic ordering of these two compounds displays a collinear antiferromagnetic ordering associated with the wavevector $\boldsymbol{q} = (001)$, corresponding to an I_P magnetic lattice with anticentring translation. The moments of all sublattices located at $(xy0)$ layers and sandwiched between successive Ag (Au) layers perpendicular to z at $z = -0.25$, 0.25 are confined to the same direction within the $(xy0)$ plane. They change their direction collectively when going to the next X layers at $z = 0.25$, 0.75. The thermal evolution of the magnetic

0953-8984/99/234469+13$19.50

intensities confirmed that the ordering temperatures are somewhat below 400 K, but also showed that the moments of the R_2 atoms located at both sites of the-non magnetic layers where the sign change takes place order at lower temperatures.

Quite different results were obtained by Yan *et al* [4] and Fangwei Wang *et al* [5] who report on the basis of neutron and x-ray data a collinear ferrimagnetic moment arrangement for the $Nd_6Fe_{13}Si$ and $Pr_6Fe_{13}Si$ compounds with the moments forming two antiferromagnetically coupled sublattices: $R_1(8f)\uparrow$, $R_2(16l)\uparrow$, $Fe_1(4d)\uparrow$, $Fe_2(16k)\downarrow$, $Fe_3(16l_1)\downarrow$, $Fe_4(16l_2)\downarrow$. The antiparallel coupling between the R moments and the net Fe moments led the authors to propose the occurrence of a compensation temperature upon cooling. These authors furthermore propose that the preferred moment direction is along ***c***, which is at variance with our previous neutron diffraction results [8]. For this reason we have extended our neutron investigation to the compound $Pr_6Fe_{13}Si$. Furthermore, in order to study the influence of a variable rare earth component on the magnetic structure, we extended our previous investigation on $Pr_6Fe_{13}Au$ to $Nd_6Fe_{13}Au$.

2. Sample preparation

The $Pr_6Fe_{13}Si$ and $Nd_6Fe_{13}Au$ samples were prepared by arc melting starting materials of at least 99.9% purity. In order to suppress the formation of compounds of the 2:17 type as far as possible we used an excess of about 2% of R. After arc melting the samples were wrapped into Ta foil, sealed into an evacuated quartz tube and annealed for about three weeks at 600 °C. After annealing the samples were quenched to room temperature by breaking the quartz tubes in water. The x-ray diffraction diagrams showed that the annealed samples were approximately single phase, their crystal structure corresponding to the tetragonal $Nd_6Fe_{13}Si$ structure type.

3. Neutron diffraction

The neutron diffraction experiments were carried out on powder samples of $Pr_6Fe_{13}Si$ and $Nd_6Fe_{13}Au$ in the temperature range 1.5–450 K. The data were collected with the D1A and D1B (double axis multicounter diffractometers) at the facilities of the ILL in Grenoble using the wavelengths $\lambda = 1.9114$ Å and $\lambda = 2.531$ Å, respectively. The step increment of the scattering angle 2θ was 0.05 or 0.1° for the D1A data, and 0.2° for the D1B data. The data were corrected for absorption and evaluated by the FullProf program [13]. The high resolution (HR) data obtained on the D1A instrument in the 2θ range 0–160° were used for structural (nuclear and magnetic) refinements for a few temperatures. The allocated beam time did not allow the use of a larger wavelength that would have made it possible to include also the first magnetic reflection in the magnetic refinements (see next sections). The data comprising the first magnetic reflection were therefore restricted to the D1B instrument. The D1B data were collected with a 5–10 K step in temperature (2θ range 2–82°) in order to derive the magnetic phase diagram only for the $Pr_6Fe_{13}Si$ compound.

3.1. Nuclear structure of $Pr_6Fe_{13}Si$ (HR 410 K data $\lambda = 1.9114$ Å)

The neutron diffraction pattern collected in the paramagnetic state at 410 K is shown in the top part of figure 1. The refined parameters, given in table 1, confirm the type of crystal structure reported earlier [1, 2]. The *R*-factor values are satisfactory and indicate no other significant deviation from the basic structure. Some foreign lines were identified to belong to a small amount (6.8%) of the hexagonal Pr_2Fe_{17} phase [14] present as impurity and were included in the refinement.

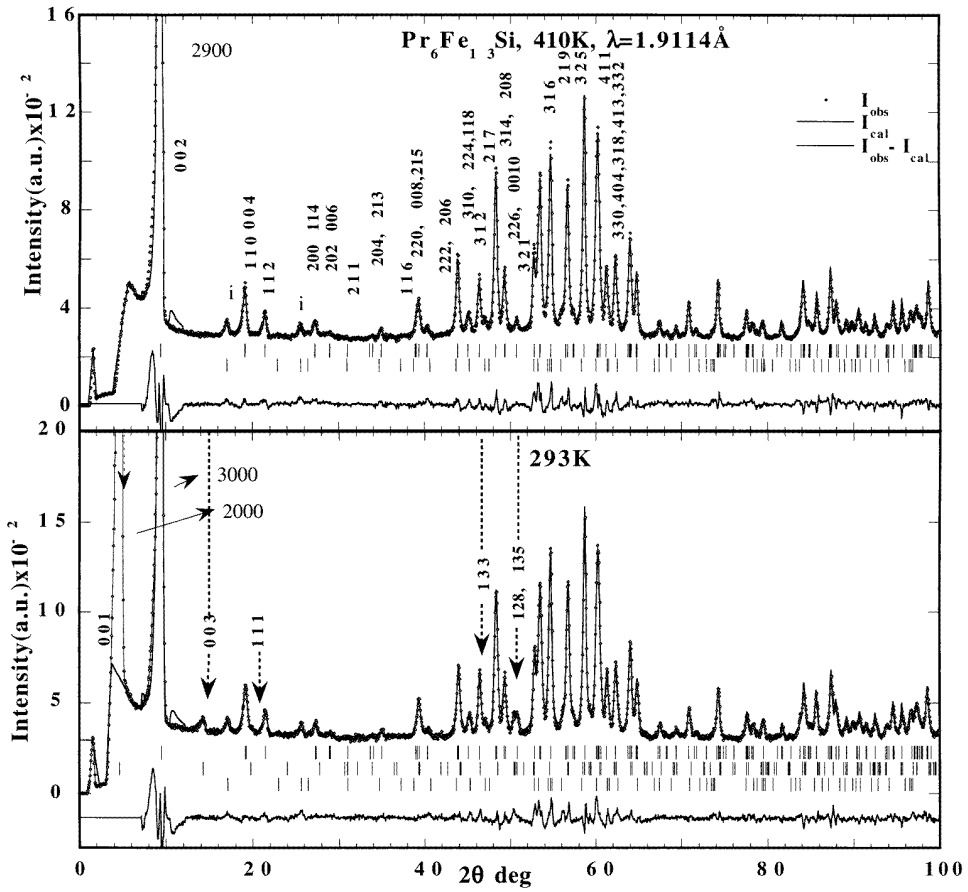

Figure 1. A part of the observed, calculated and difference neutron HR patterns (D1A diffractometer) of $Pr_6Fe_{13}Si$ in the paramagnetic state at 410 K and the magnetically ordered state at 293 K. The strongest magnetic reflections are indicated by arrows. The *hkl* indices are indicated for some of the reflections. The relative intensities of the magnetic reflections falling outside the frame of the figure have been indicated by numbers.

3.2. Magnetic ordering of $Pr_6Fe_{13}Si$ ($\boldsymbol{q} = 0, 0, 1$) HR data $\lambda = 1.9114$ Å

The major characteristic of the 293 K (D1A data) neutron patterns collected in the magnetically ordered state is the presence of a dominant (001) reflection at $2\theta = 4.8^\circ$ (see figure 1 (bottom part)). The same characteristics are also found in the D1B data collected at 110 K (see next section). The other magnetic contributions are difficult to distinguish from the nuclear reflections at higher angles. These observations in the neutron patterns of the magnetically ordered state suggest low magnetic intensity values. This can be expected to make the data analysis cumbersome, because the weak magnetic reflections may overlap with the stronger nuclear ones in view of the large lattice constants. Here we wish to mention that the dominant (001) reflection is missing in the D1A data obtained at 1.5 and 120 K (collected with another cryostat) because of the different position of the primary beam cutter.

The percentage of magnetic intensities relative to the overall intensity does not exceed 6% when the (001) reflection is excluded, but it becomes over 40% when including the (001)

Table 1. Refined structural parameters of $Pr_6Fe_{13}Si$ ($I4/mcm$) from HR neutron data in the paramagnetic state at 410 K and the magnetically ordered state at 293 K and 120 K, 80 K, 1.5 K. μ_{xy} is the refined moment component within the tetragonal plane. Included is also a refinement based on D1B (high flux data 110 K) R_n, R_m are the reliability factors for the integrated nuclear and magnetic intensities respectively. R_{wp}, R_{exp} are the reliability factors for the weighted profile intensities and of the expected weighted profile intensities respectively.

	410 K (HR, D1A)				293 K (HR, D1A)					120 K(HR, D1A)				
Atom/site	x	y	z	B [nm^2]×10^2	x	y	z	μ_{xy} [μ_B]	B [nm^2]×10^2	x	y	z	μ_{xy} [μ_B]	B [nm^2]×10^2
Pr1 8f	0	0	0.1098(5)	1.8(1)	0	0	0.1101(6)	1.1(2)	2.3(2)	0	0	0.1105(5)	2.3(2)	1.8(1)
Pr2 16l	0.1685(7)	0.6685(7)	0.1892(3)	1.8(1)	0.1672(8)	0.6672(8)	0.1898(3)	0.6(2)	2.3(2)	0.1678(7)	0.6678(7)	0.1906(3)	2.0(1)	1.8(1)
Fe1 4d	0.0	0.5	0.0	2.0(1)	0	0.5	0	1.4(2)	2.1(1)	0	0.5	0	1.0(2)	1.6(1)
Fe2 16k	0.0666(6)	0.2076(6)	0	2.0(1)	0.0678(6)	0.2084(6)	0	1.3(1)	2.1(1)	0.0676(6)	0.2078(5)	0	1.7(2)	1.6(1)
Fe3 16l$_1$	0.1768(4)	0.6768(4)	0.0609(2)	2.0(1)	0.1780(4)	0.6780(3)	0.0610(2)	1.4(2)	2.1(1)	0.1776(4)	0.6776(4)	0.0607(2)	1.9(1)	1.6(1)
Fe4 16l$_2$	0.3843(4)	0.8843(4)	0.0961(1)	2.0(1)	0.3851(4)	0.8851(4)	0.0967(2)	1.0(2)	2.1(1)	0.3853(4)	0.8853(4)	0.0971(2)	2.1(1)	1.6(1)
Si 4a	0.0	0.0	0.25	2.2(3)	0	0	0.25		2.5(3)	0	0	0.25		2.0(4)
a, c [nm]	0.805 36(2)	2.2833(1)			0.805 43(3)	2.2873(1)				0.804 74(4)	2.2823(1)			
R_n, R_m, R_{wp}, R exp (%)	5.5, —, 16, 5				5, 14, 17, 7					5, 11, 17, 6				

	80 K (HR, D1A)			μ_{xy} [μ_B]	1.5 K (HR, D1A)					110 K (D1B)				
Pr1 8f	0	0	0.1109(7)	2.6(2)	0	0	0.1097(7)	2.8(2)	1.5(2)	0	0	0.1105	2.2(4)	1.5
Pr2 16l	0.1680(9)	0.6680(9)	0.1899(4)	2.2(1)	0.1677(9)	0.6677(9)	0.1907(5)	2.7(1)	1.5(2)	0.1678	0.6678	0.1906	2.4(4)	1.5
Fe1 4d	0	0.5	0	0.8(2)	0	0.5	0	0.9(2)	1.3(1)	0	0.5	0	0.6(3)	1.5
Fe2 16k	0.0680(8)	0.2089(7)	0	1.6(2)	0.0678(8)	0.2081(7)	0	2.0(2)	1.3(1)	0.0678	0.2087	0	1.6(2)	1.5
Fe3 16l$_1$	0.1774(5)	0.6775(5)	0.0611(3)	2.0(2)	0.1775(6)	0.6776(6)	0.0608(3)	2.1(1)	1.3(1)	0.1770	0.6772	0.0611	2.0(2)	1.5
Fe4 16l$_2$	0.3858(5)	0.8858(5)	0.0973(2)	2.4(2)	0.3848(5)	0.8848(5)	0.0971(3)	2.1(1)	1.3(1)	0.3847	0.8847	0.0975	1.9(3)	1.5
Si 4a		0	0.25		0	0	0.25		1.8(6)	0	0	0.25		1.5
a, c [nm]	0.8046(4)	2.2816(2)			0.804 79(4)	2.2808 (2)				0.8050(1)	2.2816(9)			
R_n, R_m, R_{wp}, R exp (%)	5, 13, 17, 6				5, 11, 17, 6					5.5, 1.3, 9.5, 1				

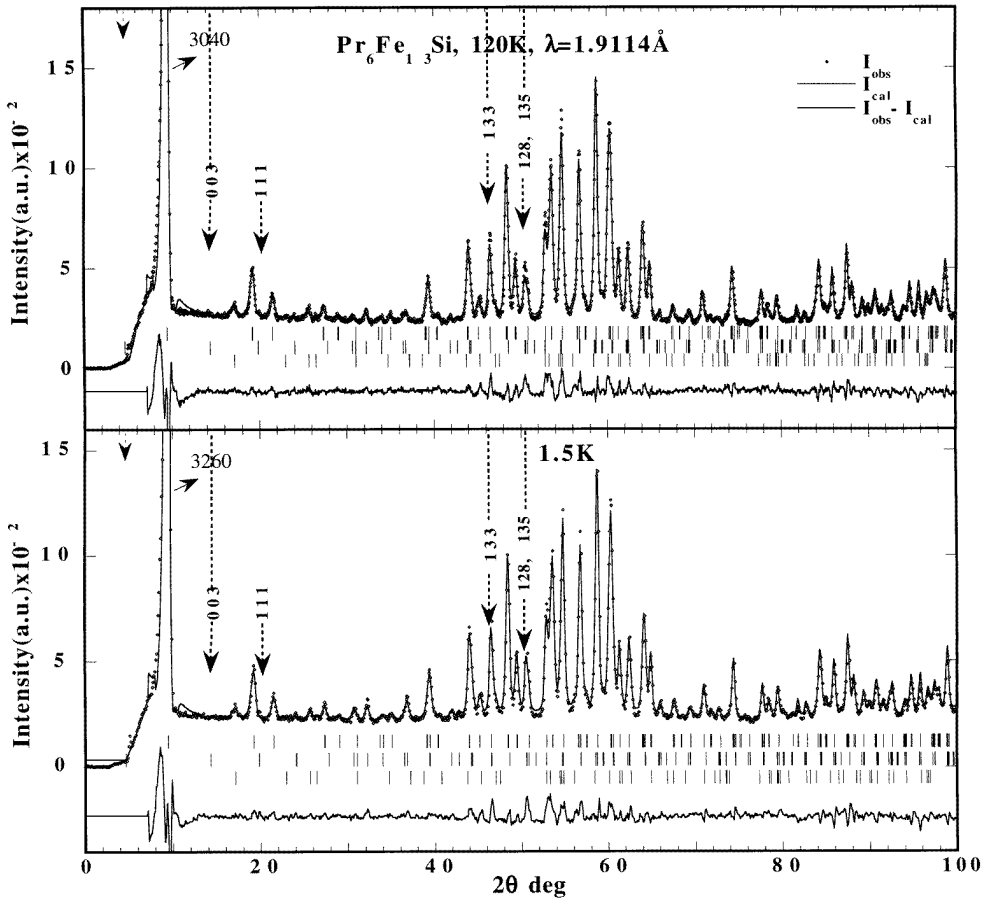

Figure 2. A part of the observed, calculated and difference neutron HR patterns (D1A diffractometer) of $Pr_6Fe_{13}Si$ in the magnetically ordered state at 120 K and 1.5 K. The strongest magnetic reflections are indicated by arrows.

reflection. A further difficulty is that the peak shape of this reflection (excluded from the refinements) is far from Gaussian due to defects of the neutron optic system of the D1A instrument and most likely a part of this reflection is reduced by the beam cutter. For similar reasons, the strong asymmetry of the first nuclear reflection cannot be fitted properly. The inclusion of the first peak in the refinements was effected only for the D1B data, shown in figure 3. The results are included in table 1 for comparison with the D1A results obtained in the same temperature range. In all D1A refinements given in the tables the (001) reflection was excluded. A further weak point in the data analysis is the difficulty of estimating the background in the high 2θ range due to the large peak overlap (large cells). This has the consequence of leading to large R_{wp} values of 16–17% for the D1A data when using the full 2θ range 7–150°.

The observation of odd (00l) reflections suggests a purely antiferromagnetic structure with the wavevector $\boldsymbol{q} = (0, 0, 1)$. The I centring condition ($h + k + l = 2n$) is not fulfilled and the magnetic lattice denoted by I_P [15, 16] has a (1/2,1/2,1/2) antitranslation. Moreover, the observed strong purely magnetic (001) intensity suggests that the main axis of antiferromagnetism is confined to the (001) plane.

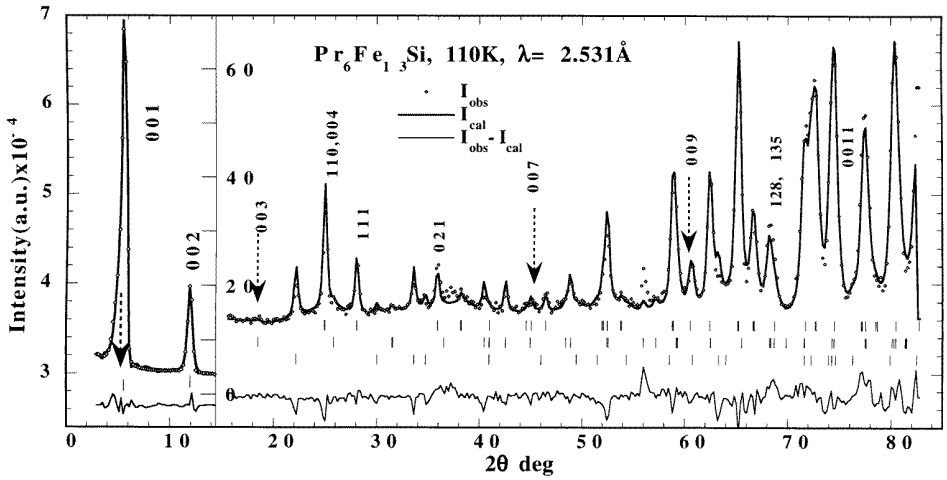

Figure 3. Observed, calculated and difference neutron high flux pattern (D1B diffractometer) of $Pr_6Fe_{13}Si$ in the magnetically ordered state at 110 K. The (00l) magnetic reflections are indicated by arrows. The low angle range (inset) is plotted in a 10× larger scale (right scale of the inset).

Symmetry analysis offers the possibility of ten magnetic space groups, eight corresponding to one-dimensional and two corresponding to two-dimensional representations. The former are identical with the eight Shubnikov groups [15, 16] listed in table 2 of [8] together with the corresponding magnetic modes. Because Pr1 at (8f) is situated on the tetragonal (00z) axis the Shubnikov groups 5–8 can be left out of consideration as they comprise a $4'$ axis which does not leave the moment of the Pr1 at 8(a) invariant. It is important to realize that none of the other groups allows a mode along x or y that may give rise to the (001) reflection. This means that there is a further symmetry lowering to one of the orthorhombic subgroups of order two not comprising a fourfold axis like $I2/m2/c21$ ($Ibam$) or $I2/m12/m$ ($Fmmm$).

In our attempt to derive in a first approximation a model for the magnetic structure we chose a fairly pragmatic way based on the observed intensities of a set of six (00l) reflections. These observed intensities were compared with calculated structure factors, that depend exclusively on the atomic z parameters (see table 3 of [8]). Due to the layered nature of the structure along z, the data analysis is simplified by the fact that there are only four atomic layers at (1) z and (2) $1/2 - z$; and their centrosymmetric counterparts at (3) $-z$ and (4) $z - 1/2$. The I antitranslation moves atoms of layer (1) $\rightarrow$ (4) and atoms of layer (2) $\rightarrow$ (3). The magnetic structure factor of the (00l) reflections of any Wyckoff site will be proportional to the expression:

$$2nf_j(\boldsymbol{m}_1 e^{-2\pi i l z} + \boldsymbol{m}_2 e^{-2\pi i l(1/2-z)} + \boldsymbol{m}_3 e^{2\pi i l z} + \boldsymbol{m}_4 e^{2\pi i l(1/2-z)}) \quad (1)$$

where the subscript 2 stands for the anticentring translation and n for 1/8 of the site multiplicity. $\boldsymbol{m}_i$ is the magnetic moment vector of a site and f_j the magnetic form factor.

For l = odd expression (1) equals:

$$2nf_j(\boldsymbol{m}_1 e^{-2\pi i l z} - \boldsymbol{m}_2 e^{2\pi i l z} + \boldsymbol{m}_3 e^{2\pi i l z} - \boldsymbol{m}_4 e^{-2\pi i l z}) \quad (2)$$

$$2nf_j(m_1 - m_2 + m_3 - m_4)\cos 2\pi l z = 8nf_j m_i \cos 2\pi l z \qquad \text{for a } (+-+-) \text{ mode along } x \quad (3)$$

$$2nf_j(-m_1 - m_2 + m_3 + m_4)\sin 2\pi l z = 8nf_j m_i \sin 2\pi l z \qquad \text{for a } (++--) \text{ mode along } y. \quad (4)$$

Table 2. Refined structural parameters of $Nd_6Fe_{13}Au$ ($I4/mcm$) from HR neutron data (D1A) in the paramagnetic state at 430 K and the magnetically ordered state at 293 K, 180 K, 120 K, 60 K and 1.5 K. μ_{xy} is the refined moment component within the tetragonal plane. R_n, R_m are the reliability factors for the integrated nuclear and magnetic intensities respectively. R_{wp}, R_{exp} are the reliability factors for the weighted profile intensities and of the expected weighted profile intensities respectively.

	430 K				293 K					180 K				
Atom/site	x	y	z	B [nm^2]×10^2	x	y	z	μ_{xy} [μ_B]	B [nm^2]×10^2	x	y	z	μ_{xy} [μ_B]	B [nm^2]×10^2
Nd1 8f	0	0	0.1100(4)	1.2(1)	0	0	0.1103(3)	2.5(1)	1.4(1)	0	0	0.1105(4)	3.2(2)	1.0(1)
Nd2 16l	0.1632(5)	0.6632(5)	0.1902(2)	1.2(1)	0.1637(3)	0.6637(3)	0.1902(2)	0.9(1)	1.4(1)	0.1638(5)	0.6638(5)	0.1903(2)	1.5(1)	1.0(1)
Fe1 4d	0	0.5	0	0.7(1)	0	0.5	0	1.5(1)	1.2(1)	0	0.5	0	1.5(2)	0.6(1)
Fe2 16k	0.0670(6)	0.2092(5)	0	0.7(1)	0.0679(4)	0.2089(3)	0	1.7(2)	1.2(1)	0.0681(6)	0.2097(5)	0	1.8(2)	0.6(1)
Fe3 16l$_1$	0.1774(4)	0.6774(4)	0.0607(2)	0.7(1)	0.1773(3)	0.6773(3)	0.0609(2)	2.0(2)	1.2(1)	0.1771(4)	0.6770(4)	0.0615(2)	2.1(2)	0.6(1)
Fe4 16l$_2$	0.3841(4)	0.8841(4)	0.0967(2)	0.7(1)	0.3841(2)	0.8841(2)	0.0980(2)	1.9(2)	1.2(1)	0.3844(4)	0.8844(2)	0.0981(2)	2.4(2)	0.6(1)
Au 4a		0	0.25	0.7(2)		0	0.25		1.6(2)		0	0.25		0.5(2)
a, c [nm]	0.808 37(3)	2.2595(1)			0.808 23(2)	2.259 05(8)				0.807 82(3)	2.255 14(8)			
R_n, R_m, R_{wp}, R_{exp} (%)	4, —, 16, 5				4, 11.3, 16, 6					4, 13, 16, 7				

	120 K			μ_{xy} [μ_B]	60 K					1.5 K				
Nd1 8f	0	0	0.1105(3)	2.9(2)	0	0	0.1108(4)	3.4(2)	1.1(1)	0	0	0.1103(3)	3.4(2)	0.45(1)
Nd2 16l	0.1638(4)	0.6638(4)	0.1905(2)	1.9(1)	0.1637(5)	0.6637(5)	0.1905(2)	2.3(1)	1.1(1)	0.1643(4)	0.6643(4)	0.1904(2)	2.5(1)	0.45(1)
Fe1 4d	0	0.5	0	1.4(1)	0	0.5	0	1.3(2)	1.0(1)	0	0.5	0	1.3(1)	0.26(3)
Fe2 16k	0667(5)	0.2089(4)	0	2.5(2)	0679(6)	0.2088(5)	0	2.2(2)	1.0(1)	0.0665(4)	0.2092(4)	0	2.6(2)	0.26(3)
Fe3 16l$_1$	0.1770(3)	0.6769(3)	0.0612(2)	2.0(2)	0.1766(4)	0.6766(4)	0.0615(2)	2.5(2)	1.0(1)	0.1773(3)	0.6773(3)	0.0614(2)	2.6(1)	0.26(3)
Fe4 16l$_2$	0.3847(3)	0.8847(3)	0.0981(2)	2.4(2)	0.3847(4)	0.8847(4)	0.0986(2)	2.6(2)	1.0(1)	0.3837(4)	0.8837(3)	0.0983(2)	2.6(1)	0.26(3)
Au 4a		0	0.25			0	0.25		1.0(2)	0	0	0.25		0.10(7)
a, c [nm]	0.808 03(4)	2.2517(2)			0.807 59(3)	2.2493(2)				0.808 00(2)	2.247 5(1)			
R_n, R_m, R_{wp}, R_{exp} (%)	5, 13, 17, 6				5, 10, 17, 7					7, 1.9, 13, 1				

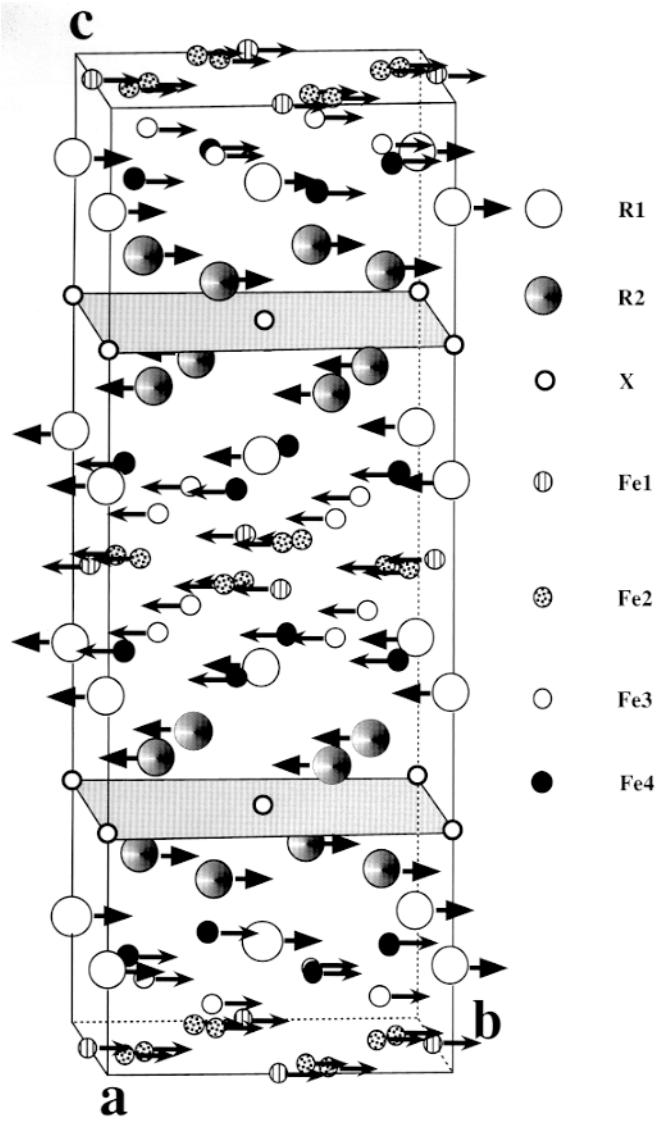

Figure 4. Schematic representation of the collinear antiferromagnetic structures in $Pr_6Fe_{13}Si$ and $Nd_6Fe_{13}Au$ with the moments confined to the (001) plane.

This analysis reveals that the (00*l*) reflections may have intensity contributions when the intralayer coupling of the moments of a given site is ferromagnetic and the interlayer moment coupling for the layers 1–4 follows the sequence (+ − +−) for the real part and (+ + −−) for the imaginary part of the structure factor. The refinement has shown that the (+ − +−) mode is in better agreement with the observations. Table 3 of [8] shows that the strong intensity of the (001) and the weak intensity of the (003) reflections are better compatible with the cosine term.

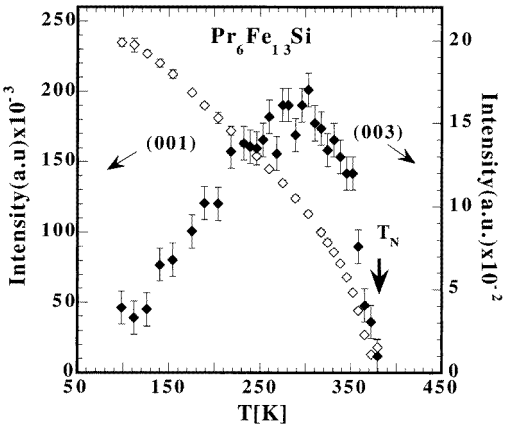

Figure 5. Temperature dependence of the integrated intensities of several (00*l*) magnetic reflections in $Pr_6Fe_{13}Si$.

3.2.1. The magnetic structure of $Pr_6Fe_{13}Si$. We mentioned already that the anticentring translation I moves an atom of layer (1) to layer (4) and an atom of layer (2) to layer (3). Simultaneously, there is a sign change of the moments of these atoms. This means that when the interlayer coupling follows the $(+-+-)$ mode (giving rise to only the cosine term in the structure factor) the intralayer coupling is ferromagnetic. Therefore, the moments of each site are arranged in four successive ferromagnetic layers coupled antiferromagnetically along $\boldsymbol{c}$ in the sequence $(+--+)$. The sign sequence refers to the layers at (1) z, (2) $1/2-z$, (4) $1/2+z$, (3) $-z$. Furthermore, the refinement has shown that the moments of the six sublattices (two for Pr and four for Fe) have their moments parallel within the (001) plane while the absolute direction relative to the $\boldsymbol{a}$ or $\boldsymbol{b}$ axes cannot be defined from powder diffraction. If the moments are parallel to the a or b axes the magnetic space group is $I_Pba'm'$ or $I_Pb'am'$, respectively. A further symmetry reduction would have to be considered for a general direction in the $(xy0)$ plane.

It is possible to give a simple description of the magnetic structure by considering that the parallel moments within the mentioned six sublattices form ferromagnetic blocks. Each of these ferromagnetic blocks is embedded between two successive non-magnetic X layers perpendicular to z located at $z = -0.25, 0.25, 0.75$. The moments in these blocks change their sign collectively when going to the next block along c. This structure is shown in figure 4.

We have summarized the refined parameters obtained for various temperatures in table 1. Apparently, the closeness of the non-magnetic X layers strongly affects the moments at the Pr2 site because our data show that these moment values are almost zero at 293 K. The Fe1 moment has the lowest average value. The other three Fe sites, within experimental error, have reached the saturation value of 2.3(1) μ_B already at 120 K. The moments of both Pr sites (2.7(1) μ_B) are still below the free ion value $gJ\mu_B = 3.2\ \mu_B$ at 1.5 K, which is most probably due to crystal field effects. Here we would like to stress that the data analysis of the weak magnetic reflections is confronted with three main problems: (a) the presence of large magnetic unit cells and a large number of free parameters, (b) the difficulty of obtaining a realistic background estimation and (c) the weak magnetic intensities overlapping with the stronger nuclear ones. These three factors leave some ambiguity as to the refined magnetic parameters which depend on the instrumental resolution. In fact, when comparing the D1B refined data obtained at 110 K and the D1A HR data obtained at 120 K one finds a slightly higher average moment value for Pr1 and a slightly lower Fe_2 moment value.

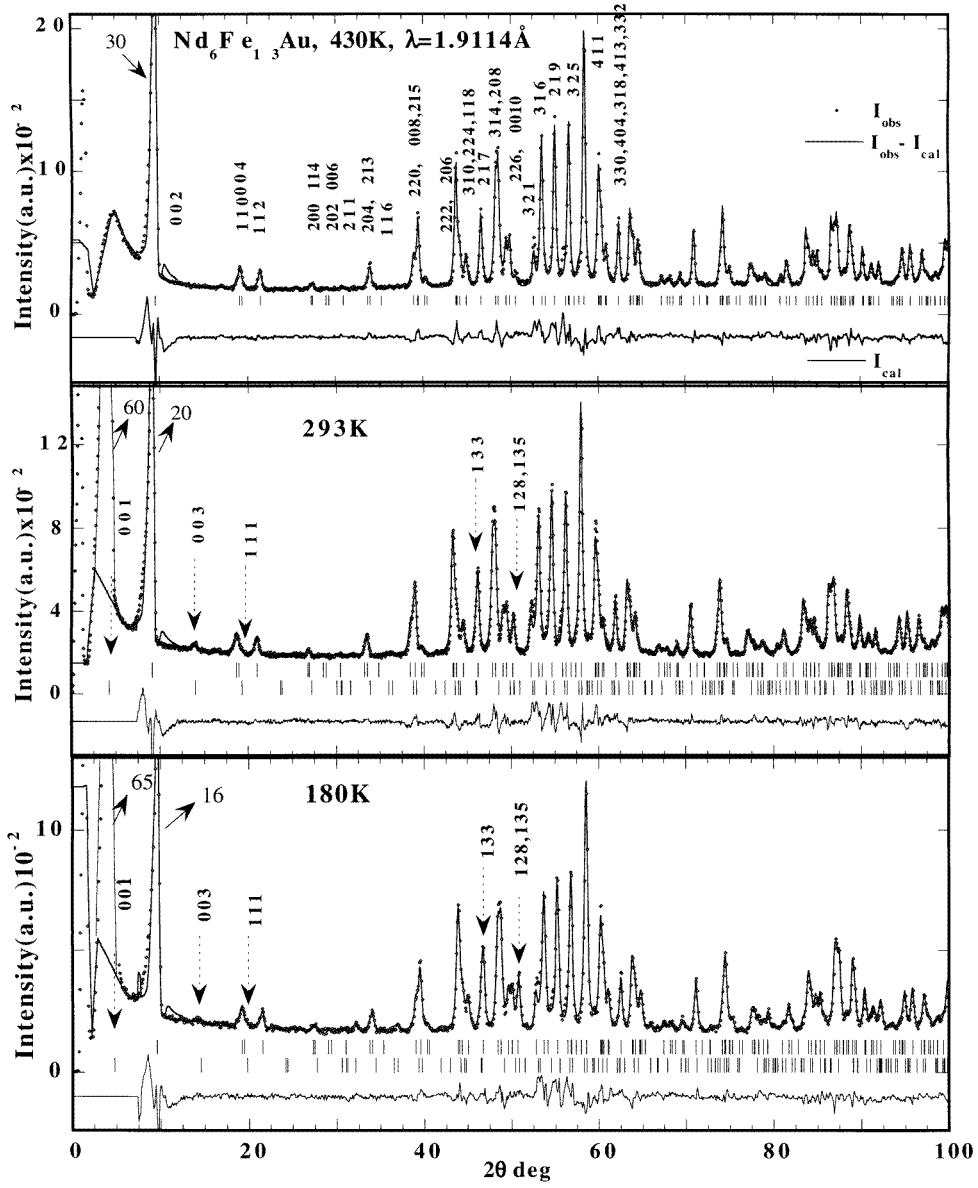

Figure 6. A part of observed, calculated and difference neutron HR patterns (D1A diffractometer) of $Nd_6Fe_{13}Au$ in the paramagnetic state at 430 K and the magnetically ordered state at 293 K and 180 K. The strongest magnetic reflections are indicated by arrows.

3.2.2. Temperature evolution of the magnetic order in $Pr_6Fe_{13}Si$. The temperature dependence of the intensity of the (001) and (003) magnetic reflections in $Pr_6Fe_{13}Si$ is shown in figure 5. A similar temperature dependence has also been observed for $Nd_6Fe_{13}Au$ to be discussed below. For the compound $Pr_6Fe_{13}Si$ magnetic order occurs at 385 ± 5 K as can be seen from the increase of the intensities of both reflections with decreasing temperature in the range 400–300 K. It can be seen in figure 5 that the intensity of the (003) reflection starts to

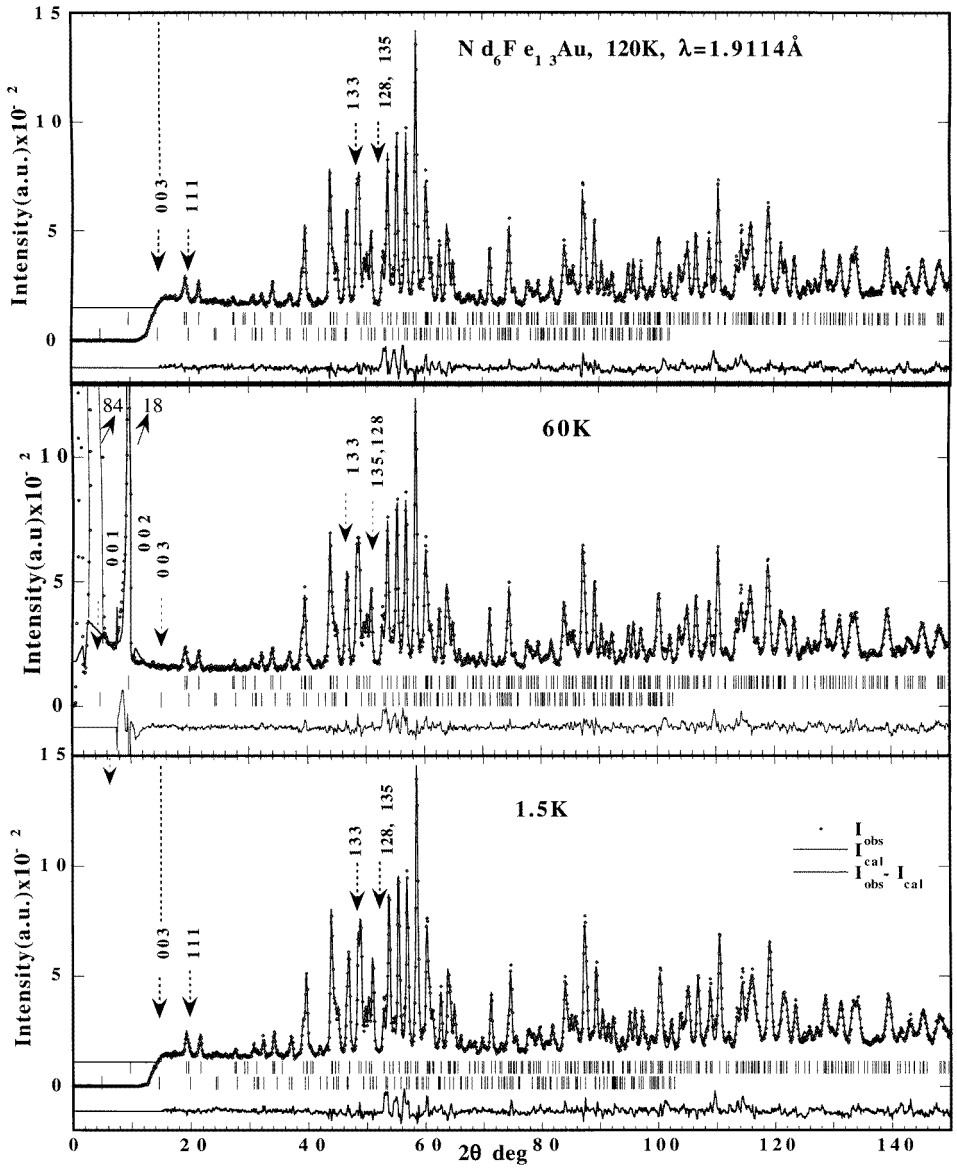

Figure 7. A part of observed, calculated and difference neutron HR patterns (D1A diffractometer) of $Nd_6Fe_{13}Au$ in the magnetically ordered state at 120, 60 and 1.5 K. In the 120 and 1.5 K data the first magnetic peaks are missing because of the primary beam stop. The strongest magnetic reflection (001) is only shown at 60 K.

decrease below about 300 K and almost vanishes below 100 K. This behaviour can be easily explained by a close inspection of the structure factor for the (003) reflection which is given by

$$-8f_{Pr}(0.482m_{Pr1} + 2 \times 0.916m_{Pr2}) \\ +4f_{Fe}(m_{Fe1} + 4m_{Fe2} + 4 \times 0.409m_{Fe3} - 4 \times 0.264m_{Fe4}). \quad (5)$$

The contributions of Pr and the contributions of the three Fe sublattices have opposite signs. As the contribution of Pr2 is four times larger than that of Pr1 it is plausible to a assume that the decreasing intensity of the (003) reflection with decreasing temperature below 300 K is due to gradual ordering of the Pr2 moments. This is in good agreement with the almost zero refined moment value for the Pr2 atom at 293 K.

3.3. The magnetic structure of $Nd_6Fe_{13}Au$

The magnetic structure of $Nd_6Fe_{13}Au$ has basically been determined along the same lines as described above for $Pr_6Fe_{13}Si$. Data obtained on the D1A instrument at a few relevant temperatures are displayed in figures 6 and 7. When comparing these data with the results shown for $Pr_6Fe_{13}Si$ in figures 1 and 2 one may notice that the magnetic intensity contributions in the low temperature region for these two compounds are virtually the same. The refined structural parameters of $Nd_6Fe_{13}Au$ are listed in table 2. In view of the close similarity between the results obtained for both compounds and the limited allocated beam time we have not studied the temperature dependence of magnetic ordering in $Nd_6Fe_{13}Au$ for the full temperature range. However, one can verify in the neutron pattern presented for the temperatures selected in figures 6 and 7 that the (003) line marking the onset of the R_2 ordering is only visible in the 293 and 180 K data and not at 60 K. This behaviour agrees with that of $Pr_6Fe_{13}Si$ shown in figure 5 and confirms that the magnetic ordering behaviour of both compounds is essentially the same.

4. Discussion

We mentioned already in section 3 that a major characteristic of the neutron patterns collected at various temperatures in the magnetically ordered state (including 295 K) is the presence of a dominant (001) reflection at $2\theta = 4.8^\circ$, and that the total intensity of the remaining magnetic contributions is lower by about an order of magnitude and is difficult to distinguish from the nuclear intensities at higher angles. The observation of this strong (001) reflection, occurring at scattering angles lower than the equally strong nuclear (002) reflection, is therefore essential for an accurate determination of the magnetic structure of the compounds. In the neutron study of Yan *et al* [4] the corresponding low angle region was excluded from measurements. The fact that the dominant (001) reflection was not included in the structural refinement of these authors is most likely the reason for the discrepancy between their results and ours.

Several $Nd_6Fe_{13}X$ compounds have been investigated by Mössbauer spectroscopy. The spectra were analysed with subspectra of relative intensities corresponding to the crystallographic structure reported in [1] and [2] without relying on a specific magnetic structure. For the compound $Nd_2Fe_{13}Au$ the easy magnetization direction was found [10, 12] to be perpendicular to the *c* axis, which is in concord with the easy magnetization direction observed for this compound in the course of the present investigation.

The preferred moment direction in $Pr_6Fe_{13}Si$ at room temperature was determined by Fangwei Wang *et al* [5] by x-ray diffraction on a magnetically aligned sample. From the fact that only (00*l*) refections were observed in their x-ray diffractogram they concluded that the preferred moment direction is parallel to the *c* axis at room temperature, a conclusion that is in obvious contrast with the results of the present neutron diffraction study. However, one has to take account of the fact that the net magnetization in these materials is extremely low because of the mutually compensating contributions of the antiferromagnetically ordered sublattices (Fangwei Wang *et al* report a value of 0.3 μ_B per formula unit for the spontaneous moment at 1.5 K). Based on the magnetic structure shown in figure 4, a net magnetization

can be induced by an applied field but may occur in a direction perpendicular to the preferred moment direction, as is commonly observed in antiferromagnetic systems. In other words, powder particles subjected to an alignment field of 10 kOe will become oriented with their *c* axis parallel to the alignment field although the preferred moment direction is perpendicular to the *c* axis. For this reason we do not consider the results of Fangwei Wang *et al* as being in conflict with the currently determined preferred moment direction in $Pr_6Fe_{13}Si$.

References

[1] Allemand J, Letand A, Moreau J M, Nozières J P and Perrier de la Bâthie R 1990 *J. Less-Common Met.* **166** 73
[2] Weitzer F, Leithe-Jasper A, Rogl P, Hiebl K, Rainbacher A, Wiesinger G, Friedl J and Wagner F E 1995 *J. Appl. Phys.* **75** 7745
[3] Sichevich O M, Lapunova R V, Soboley A N, Grin Yu N and Yarmoluk Ya P 1985 *Sov. Phys.–Crystallogr.* **30** 627
[4] Yan Q W *et al* 1994 *J. Phys.: Condens. Matter* **6** 3101
[5] Wang Fangwei, Shen Bao-Gen, Gong Huayong, Sun Xiangdong, Zhang Panlin and Yan Qiwei 1998 *J. Magn. Magn. Mater.* **177–181** 1056
[6] Hu Bo-ping, Coey J M D, Klesnar H and Rogl P 1992 *J. Magn. Magn. Mater.* **117** 225
[7] de Groot C H, de Boer F R, Buschow G H J, Hautot D, Long G J and Grandjean F 1996 *J. Alloys Compounds* **233** 161
[8] Schobinger-Papamantellos P, Buschow K H J, de Groot C H, de Boer F R, Ritter C, Fauth F and Boettger G 1998 *J. Alloys Compounds* **280** 44
[9] Kajitani T, Nagayama K and Umeda T 1992 *J. Magn. Magn. Mater.* **117** 379
[10] Hautot D, Long G J, Grandjean F, de Groot C H and Buschow K H J 1998 *J. Appl. Phys.* **83** 1554
[11] de Groot C H, Buschow K H J and de Boer F R 1998 *Phys. Rev.* B **57** 11 472
[12] Wiesinger G, Rainbacher A, Steiner W, Leithe-Jasper A, Rogl P and Weitzer F 1994 *Hyperfine Interact.* **94** 1915
[13] Rodríguez-Carvajal J 1993 *Physica* B **192** 55 The manual of FullProf can be obtained from a Web browser at `ftp://bali.saclay.cea.fr/pub/divers/fullp/doc`
[14] Isnard, Miraglia S, Soubeyroux J L, Fruchart D and Pannetier J 1992 *Phys. Rev.* B **45** 2920
[15] Koptzik V A 1966 *Shubnikov Groups* (Moscow: Moscow University Press)
[16] Opechowski W and Guccione R 1965 *Magnetism* vol IIA, ed G T Rado and H Suhl (London: Academic) ch 3, p 105